The Use of Photomultiplier Tubes for Photon Counting

R. Foord, R. Jones, C. J. Oliver, and E. R. Pike

A number of photomultiplier tubes have been assessed for application in experiments where the counting of individual photoelectrons from the photocathode is necessary or advantageous. Pulse height distributions, signal-to-noise-in-signal ratios, over-all quantum-counting efficiencies, time dependent statistical correlations, and dark current properties have been investigated and compared with theoretical expectations. A major finding has been the general low value of over-all quantum-counting efficiency. Direct measurements of this figure have not, to our knowledge, been published previously. A second conclusion has been that, although there seems to be no reason why high performance with respect to each of the features considered should not be achieved in a single tube, we have not yet found one in which this is so.

I. Introduction

The photomultiplier tube is a device in which an incident (optical) electromagnetic field ejects single photoelectrons from a photocathode which are then multiplied by a cascaded secondary emission process to produce pulses of charge at the anode. At high light levels, these pulses will overlap and a measurement of anode current gives the required measure of incident light intensity; at lower light levels, however, the greatest amount of information is obtained when the photomultiplier is used in such a way that the individual photoelectrons from the photocathode are detected (i.e., by photon counting). Less information is lost by handling the information digitally, since this removes, to a first approximation, the effects of gain instability which are marked in analog uses of photomultipliers; in addition, electrons arriving at the anode not originating from the cathode can be discriminated against with a consequent improvement in signal-to-noise ratio.

The results that we present have been accumulated over some three years of work in our laboratory on the statistical properties of optical fields, particularly on direct and scattered He–Ne laser light. Most of this work has, therefore, made use of S–20 cathode tubes, but the general principles of operation will not differ appreciably with cathode type, and we feel that much of what we have learned in this very stringent application of the photomultiplier tube will be of general interest.

Many photomultipliers of an advanced type have been designed for use, together with scintillators, as detectors in nuclear physics experiments. The significant difference between this usage and that with optical radiation is that in the former case, many photons are produced in the scintillator for each incident particle, whereas only single photons are involved in the latter case. Provided that enough photons are produced in the scintillator, the effect of the cathode quantum efficiency and the collection efficiency will be merely to reduce the apparent gain of the system since the majority of incident particles will actually produce an output pulse. In counting single photons, however, a much poorer relationship between signal in and pulses out is obtained. Since the over-all quantum-counting efficiency plays such an important role in determining the performance of photomultiplier tubes, it is considered in some detail.

We might mention here that the question of energy resolution, which concerns the ratio of the amount of charge in the output pulse to the number of photons produced in the scintillator, is relatively unimportant in the detection of optical radiation since lack of energy resolution affects only the threshold setting chosen to discriminate against pulses not originating at the photocathode. A new tube having a greatly increased secondary emission ratio at the first dynode has re-

The authors are with the Royal Radar Establishment, Malvern, Worcestershire, England.

Received 12 November 1968.

cently been introduced by RCA. This development will have the effect of improving the energy resolution of the photomultiplier when used with a scintillator as a particle detector; it may also improve the photomultiplier as a detector of single photons. However, we have not yet had the opportunity to evaluate it. Improvement would chiefly result from a possible slight increase in collection efficiency corresponding to a reduced probability of pulses being lost between the first and second dynodes, and also a possible decrease in transit time spread if the number of dynodes can be reduced.

In Sec. II, we consider the theoretical description of the behavior of a photomultiplier tube. In Sec. II.A, theoretical forms of the pulse height distribution are considered. Some authors observed distributions following simple theoretical predictions,[1-6] others obtain a quasi-exponential form for the pulse height distribution[2,7-14]; to explain these latter distributions, a more complicated theory is required.[15] In Sec. IV, the pulse height distributions for various tubes are measured and compared with theory.

The effect of quantum efficiency on noise-in-signal is derived in Sec. II.B and II.C and compared with measurements in Sec. V. In Sec. V, the collection efficiency, photocathode quantum efficiency, and overall quantum-counting efficiency are assessed by several mutually independent techniques, and the results are compared with those obtained using the conventional methods proposed by the IRE (1962).[16] Measurements of either collection efficiency or noise factor based on methods similar to the IRE standards have been made.[4,17-21,43]

In Sec. III, we deal with experimental techniques. Such considerations as the construction of the base resistor chain (Sec. III.B), the choice of amplifier (Sec. III.C), and the use of discriminators and counters (Sec. III.D) are discussed, and some indications are given of distorting effects these may introduce.

In Sec. VI, time dependent correlations in the photomultiplier output are considered. It is known that correlations have a considerable effect on the tube noise and hence in particular, on the tubes usefulness for the study of correlations in light fields.[22,23] In Sec. II.D, the theoretical background to these correlation measurements is outlined.

In Sec. VII, the dark count properties of photomultiplier tubes are considered. Measurements of the temperature dependence of the dark count rate (Sec. VII. A), the pulse height distribution (Sec. VII.B) and the time dependent properties (Sec. VII.C) of the dark counts are given. In Sec. VIII, various conclusions are drawn about photomultiplier tube performance in each of the aspects which have been discussed previously.

II. Theory

A. The Pulse Height Distribution

Photoelectrons incident on the first dynode give rise to a cascade, secondary emission process yielding output pulses at the anode of 10^6–10^8 electrons. The gain of the system (electrons out/single electron in) is not a fixed quantity but varies statistically in a manner determined by the secondary emission process. This variation in gain can be studied by considering the charge distribution of the output pulses (pulse height distribution).

The secondary emission process has generally been assumed to follow Poisson statistics.[15,24-27] Woodward[25] derived expressions for the moments of the pulse height distribution after r stages of multiplication. In particular, the mean and the variance are given by

$$\langle n_r \rangle = \mu^r, \tag{1}$$

$$\mathrm{var}(n_r) = \mathrm{var}(n_1)\mu^{r-1}[(\mu^r - 1)/(\mu - 1)], \tag{2}$$

where n_r is the number of electrons at the rth dynode for a single electron input, and μ is the mean gain per stage. If one assumes that the secondary emission process follows Poisson statistics, then

$$\langle n_1^2 \rangle = \langle n_1 \rangle = \mu, \tag{3}$$

and so

$$\langle n_r^2 \rangle = \mu^r[(\mu^r - 1)/(\mu - 1)]. \tag{4}$$

The relative variance,

$$\Delta = \mathrm{var}(n_r)/\langle n_r \rangle^2, \tag{5}$$

is then given by

$$\Delta = \frac{1}{\mu^r}\left(\frac{\mu^r - 1}{\mu - 1}\right) = \left(\frac{1 - \mu^{-r}}{\mu - 1}\right). \tag{6}$$

In the limit for $r \gg 1$, we have for $\mu \gg 1$,

$$\Delta \sim 1/\mu \tag{7}$$

and for $\mu \ll 1$,

$$\Delta \sim 1/\mu^r. \tag{8}$$

Equation (7) was derived by Woodward and corresponds to a gaussian pulse height distribution. Equation (8) corresponds to a Poisson distribution. Theoretically, therefore, for a large number of stages, the pulse height distribution should lie between Poisson ($\mu \ll 1$) and gaussian ($\mu \gg 1$) limits. Computer calculations of the predicted distributions for various values of μ and r have been performed, assuming Poisson statistics.[15,27] In order to explain observed quasi-exponential pulse height distributions, Baldwin and Friedman[12] developed a theory in which the secondary emission distribution is the geometric (Furry) distribution:

$$P(n) = \mu^n(\mu + 1)^{n+1}. \tag{9}$$

Prescott[15] has analyzed the process assuming Poisson secondary emission statistics but allowing for a spread of gain across the dynode surfaces. He introduces the negative binomial (Polya) distribution:

$$P(n) = \binom{n + s - 1}{n}(\mu/s)^n(\mu/s + 1)^{-s-n} \tag{10}$$

for the model of the dynode statistics, with a parameter $s(= 1/b)$ describing the excess variance due to dynode inhomogeneities. Under these conditions, the observed variance, after r stages where $r \gg 1$, is given by

$$\mathrm{var}(n_r) = [(b\mu + 1)/(\mu + 1)]\mu^2. \tag{11}$$

For $b = 0$, this is identical to Poisson statistics, and for $b = 1$, to Furry statistics. From a comparison of the observed variance with that expected for Poisson statistics, estimates can be made of the dynode inhomogeneities.

B. The Noise Spectrum

When a photocathode is illuminated, there is a certain probability per incident photon, called the quantum efficiency η, that a photoelectron will be emitted. Not all the electrons leaving the cathode give rise to pulses at the anode, and a parameter F, generally called the collection efficiency, needs to be introduced to allow the possibility of a cascade not occurring. Thus the output of the photomultiplier resulting from samples of m incident photons per second will be, on average, $\langle n \rangle$ pulses per second, where

$$\langle n \rangle = m\eta F. \tag{12}$$

An over-all quantum-counting efficiency α can be defined by the relation:

$$\alpha = \eta F. \tag{13}$$

The noise spectrum is calculated as follows:

Suppose a train of pulses is studied for an integration time T, which is divided into N consecutive intervals of duration τ. If each pulse has the normalized shape $h(t)$, then the charge arriving at the multiplier output in the kth interval is given by

$$Q_k = \sum_r q_r Y_r h[(k - r)\tau], \tag{14}$$

where q_r and Y_r are independent random variables; q_k describes the variation of charge per pulse and Y_k describes the probability of a pulse being present with $h(0)$ at k.

The spectral density, therefore, is given by

$$S_T(\Omega) = \left\langle \frac{1}{N\tau} \left| \sum_{k=0}^{N} Q_k\, e^{i\Omega k\tau} \right|^2 \right\rangle \tag{15}$$

$$= \left\{ \frac{1}{N\tau} \sum_{j,k=0}^{N} \sum_{r,s=0}^{N} q_r q_s^* Y_r Y_s^* h[(k - r)\tau] h^* [(j - s)\tau] \exp[i\Omega(k - j)\tau] \right\}. \tag{16}$$

If the diagonal and nondiagonal elements are separated, the spectrum can be easily shown to be

$$S_T(\Omega) = |G(\Omega)|^2 [\langle n \rangle \langle q^2 \rangle + \langle q \rangle^2 \langle n \rangle^2 \delta(\Omega) N\tau], \tag{17}$$

where $G(\Omega)$ is the Fourier transform of $h(t)$. The second term is a dc component depending on the integration time, and the first term shows how the Schottky formula must be generalized to allow for variations in gain.

Some spectrum analyzers do not measure the rms voltage of a random signal, but measure the mean value over the integration time (reciprocal bandwidth). The observed spectrum is then given by

$$S'_T(\Omega) = \left\langle \frac{1}{N\tau} \left| \sum_{k=0}^{N} Q_k e^{i\Omega k\tau} \right| \right\rangle, \tag{18}$$

which differs from the square root of the spectral density [Eq. (15)]. Care must, therefore, be taken in making sure that S and not S_T' is measured.

C. Signal-to-Noise-in-Signal Ratio

From Eq. (17), the rms noise voltage in a frequency band Δf developed across a load resistance R is given in the low frequency region by

$$V_N = eR(2m\eta F \langle g^2 \rangle \Delta f)^{\frac{1}{2}}, \tag{19}$$

since $\langle q^2 \rangle = e^2 \langle g^2 \rangle$ and $G(0) = 1$. The signal is given by

$$V_S = eRm\eta F \langle g \rangle. \tag{20}$$

Therefore the signal to noise-in-signal ratio is given by

$$\frac{V_S}{V_N} = \left(\frac{m\eta F}{2\Delta f} \frac{\langle g \rangle^2}{\langle g^2 \rangle} \right)^{\frac{1}{2}}, \tag{21}$$

and since $\mathrm{var}(g) = \langle g^2 \rangle - \langle g \rangle^2$, we find that

$$\frac{V_S}{V_N} = \left(\frac{m\eta F}{2\Delta f} \right)^{\frac{1}{2}} \left[1 + \frac{\mathrm{var}(g)}{\langle g \rangle^2} \right]^{-\frac{1}{2}}. \tag{22}$$

Thus the signal to noise-in-signal ratio is a function of the photocathode quantum efficiency, the multiplier collection efficiency and the shape of the gain distribution, which is equivalent to the single-electron pulse height distribution. However, if the output of the multiplier were standardized in a discriminator, so that $\mathrm{var}(g) = 0$, then the effect of the gain distribution would be removed. Generally, it is the apparent gain of the multiplier, not the actual gain, that is measured. The apparent gain at a given voltage is given by

$$g_{app} = \frac{\text{anode radiant sensitivity}}{\text{cathode radiant sensitivity}}. \tag{23}$$

The true gain g is related to g_{app} by the equation:

$$g_{app} = Fg. \tag{24}$$

Replacing g by g_{app} in Eq. (22) does not alter the dependence of V_S/V_N on F.

D. Time-Dependent Statistics

We have referred earlier to the use of the photomultiplier tube in the measurement of the statistical properties of light fields. The most widely used technique has been to measure the photon counting distribution,[22] $p(n,T)$; this is the probability that n photoelectrons will be detected in a time T. The factorial moments of the photon counting distribution yield information on the higher order optical correlations of a light field. In particular, it has been shown to great accuracy[28] that

for coherent radiation, the distribution is Poisson with normalized factorial moments:

$$n^{(r)} = 1, \tag{25}$$

while for ideally incoherent radiation, the normalized factorial moments are given by

$$n^{(r)} = r!. \tag{26}$$

A bibliography of recent theoretical results in the statistics of various optical fields can be found in Jakeman and Pike.[29] Measurements of the normalized factorial moments with sample times of the order of $(\Delta\nu)^{-1}$ have been used in the determination of optical line width $\Delta\nu$ (Ref. 30), and statistical measurements of a similar kind have been widely used to study the properties of laser light near the threshold of operation.[23,31,32]

These measurements are all dependent on the photomultiplier tube not introducing correlations into the distribution. Measurements of $p(n,T)$ can be used to investigate the presence of correlations in the photodetector if the incident radiation is known to be coherent (uncorrelated distribution). This technique has been used to investigate the properties of photomultiplier tubes by Oliver and Pike.[6] Correlations are also observed if the dark current pulses are not emitted at random. Since correlations in the output for coherent illumination or for the dark current means a greater variance in the signal, this implies worse detectability of small modulations or weak signals than in the ideal, random situation. Correlations also clearly render those multipliers which suffer from them less useful for statistical photon counting measurements.

III. Apparatus and Experimental Procedure

A. Photomultiplier Tubes Studied

In this paper the properties that have been discussed theoretically in Sec. II are investigated for the following S–20 cathode photomultiplier tubes:

EMI	9558B, 9658A,* D22498,*
ITT	FW 130
Mullard	56 TVP,*
RCA	7265, C70045C

B. Base Arrangement

Since the photomultiplier is a charge generating device, the output is best fed into a short circuit. Some authors[33] have used high impedance output circuitry. The stray capacitance of the anode then has to discharge through this high impedance giving a long time-constant back edge to the pulse. Pulse pile-up can then occur unless the output is shaped by clipping. In this work it was found convenient to have the amplifier separated from the photomultiplier base, and so a short length of 50 Ω cable, matched at both ends to reduce reflection, was used instead of a short circuit.

It is important that the base design should give the optimum pulse shape. Variation in the position of the same components was found to alter the pulse counting properties of these tubes considerably, through changing the pulse shape. Much care therefore has to be taken in the design of the base to achieve the results described here. In some cases, poor base construction was responsible for the pulse height distribution varying from near-exponential to near-Poisson statistics. In the former case, reflections and rings following larger pulses dominate the low end of the pulse height distributions.

C. Amplifiers

Amplifiers used in conjunction with photomultipliers need to possess the following properties: (i) rise time comparable with that of the photomultiplier, (ii) gain sufficient for the combined gain of tube and amplifier to give sufficient response to single electrons, and (iii) low distortion or correlations in use. In the light of these essentials, it should be pointed out that, generally speaking, the photomultiplier itself provides the best high gain, wide band amplification. Contrary to generally accepted practice, it is advisable to operate the tube at high supply voltages and to use minimum external amplification. Provided that cold field emission or ionization do not take place in the tube under these circumstances, this provides the best division of gain. It was found in most cases that amplifiers introduced distortion and correlation into the photomultiplier signal to a much greater extent than the multiplier itself up to extraordinarily high voltages. Conventional practices with respect to the optimization of signal-to-noise ratios for current operation need to be carefully reviewed for photon counting.

In this work, the photomultiplier gains lie in the 10^6–10^8 range, and, when used with amplifiers with gains of 10–100, give the necessary pulse height to exceed the threshold levels of modern tunnel diode discriminators.

We have tried many amplifiers for this purpose and the best we have found to date is the design by Jackson.[34] This circuit has a 1-nsec rise time and admirable overloading characteristics, so much so, in fact, that we use it deliberately in its saturated mode over most of the output distribution of the multiplier, thereby improving our dynamic range by a large factor. We explain in Sec. IV how to obtain distributions under these conditions.

D. Discriminators and Scalers

It is important that the over-all gain of the combined photomultiplier–amplifier system should be kept as low as possible, since increased gain is always obtained at the expense of bandwidth. Thus, the discriminator should be used always at maximum sensitivity. For this work a Harwell 2000 series 100-MHz discriminator

* We are grateful to the manufacturers for the loan of these tubes for evaluation.

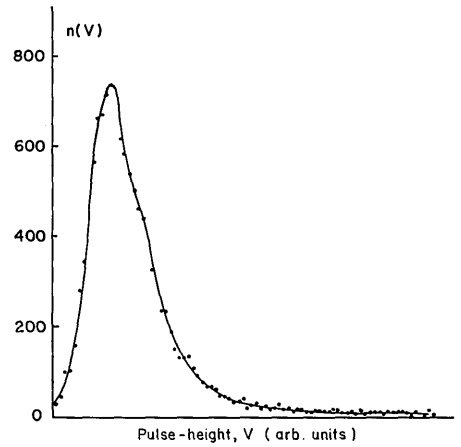

Fig. 1. A pulse height distribution (SER) for an EMI 9558B photomultiplier tube obtained using an amplifier and a multichannel pulse height analyzer.

was operated with the minimum threshold of 2 mA into 50 Ω. This discriminator was gated by a sample time pulse in order to measure the p (n,T) probability distribution. This resulted in some pulses being clipped by the inhibit signal and so a second similar discriminator was used to provide standard width pulses to the counting equipment.*

The discriminator fed a Harwell 2000 series 300-MHz scaler board from which the output was decoded into a bank of 1-MHz scalers used as a fast store by a method similar to that described by Johnson *et al.*[22] The input circuit of the scaler was carefully designed and adjusted to have the same sensitivity, whichever state the first binary stage was in; if this were not the case an odd-even bias would appear in the photon-counting distributions due to the residual marginal pulses from the discriminators.

For all pulse measurements described in this paper, the same electronic circuitry was used, so that all properties were measured under operating conditions identical to those in photon counting experiments.

IV. Measurement of Pulse Height Distribution

Each photomultiplier cathode was illuminated with 6328-Å radiation from a Spectra-Physics 119 He–Ne laser. The pulse height distribution was investigated using a fixed 2-mA threshold level and measuring the count rate as a function of the tube voltage for a suitable fixed amplifier gain. The density function (change in count rate with voltage) measured in this fashion differs from a conventional differential bias curve in that the relative width, as well as the peak position, depends on the supply voltage. If an analytic form, based on Prescott's analysis,[15] is assumed for the pulse height distribution, then the expected density function can be obtained by calculating the pulse height distribution for each value of over-all tube gain as the supply voltage is altered. For each tube gain, the area of the distribution above the fixed discriminator levels corresponds to a point of the density function. The variation in the over-all gain of the tube as a function of the supply voltage can be measured from the dependence of the output current on supply voltage. In this work, comparison of the observed density function with that expected assuming Poisson statistics is used to obtain a value of the parameter b (Ref. 15), and hence the nearest analytic form to the observed distribution.

To measure the conventional pulse height distribution, one of two methods is adopted: either the photomultiplier output could be further amplified and fed into a multichannel analyzer, or the discriminator threshold could be varied. In the first case, a differential bias curve (single electron response, SER), i.e., pulses within small range of pulse height, would be obtained. In the second case, an integral bias curve, i.e., pulses above a certain pulse height, would be obtained. These methods have certain disadvantages, however, which render them unsuitable for measurements with fast tubes having low dead times. The first method would be limited by the dead time of the multichannel analyzer used (typically $\sim$ 10 μsec); correlated after-pulses occurring within this period would not be detected. Thus no estimate of pulse width, or of the presence of correlated after-pulses, could be made in this way. A measurement of the SER using a multichannel analyzer is of use, provided that it is not necessary to use dead times shorter than that of the analyzer in subsequent experiments. Both methods of measuring the pulse height distribution involve the use of amplifiers having a larger dynamic range ($\sim$50:1) than is necessary; a condition that again can only be obtained at the expense of bandwidth. Tests using the photon-counting equipment, revealed that all amplifiers introduced measurable correlations, even without the requirement of large dynamic range. Thus, although the method adopted here does not yield the conventional SER, it is the method most compatible with the requirements of photon counting.

An SER for an EMI 9558B, measured in the conventional way using amplifiers and a multichannel pulse height analyzer, is illustrated in Fig. 1. Though less reliance can be placed on distributions obtained in this manner than on those measured by varying the supply voltage, for reasons which have been summarized above, the distribution illustrates at least qualitative agreement with the predictions of Poisson secondary emission statistics. This can be compared with the results of Gadsden[13] for an EMI 9558A which give virtually an

* It is never possible to eliminate completely discriminator output pulses which are of marginal height with respect to the threshold of the following scaler; we have, on occasion, used three discriminators in series.

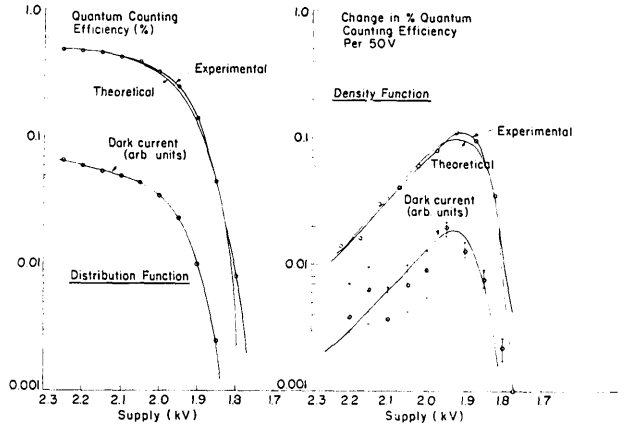

Fig. 2. Distribution and density functions for an ITT FW 130 photomultiplier tube obtained by varying the tube voltage and measuring the count rate above a fixed threshold. Both light and dark count rate distributions and the theoretical predictions, assuming Poisson multiplication statistics, are shown.

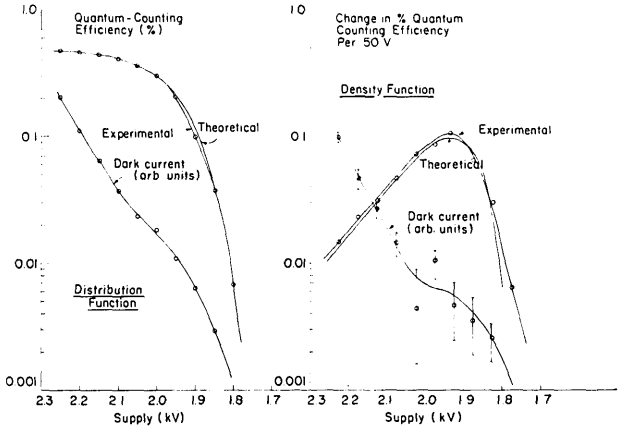

Fig. 3. As in Fig. 2 for a second ITT FW 130 photomultiplier tube.

exponential dependence. In fact, if a tube is arbitrarily hooked up to a multichannel analyzer via a commercial amplifier, the most likely result will be an exponential SER. It is only when good high frequency techniques are employed, with due regard to the large dynamic range of pulses present, that large distortions can be avoided.

Figures 2 and 3 illustrate the integral and differential distributions for two ITT FW 130 photomultipliers measured by varying the supply voltage. In addition, calculated distributions, assuming the observed gain per stage, are included showing excellent agreement. The integral and differential distributions for the EMI 9558B, 9658A, and D22498 are shown in Fig. 4; those for the Mullard 56TVP are shown in Fig. 5. The distributions for the 56 TVP were obtained using two different arrangements of the same decoupling capacitors on the last dynode. As can be seen, construction played an important role in determining the effectiveness of the photomultiplier in photon-counting applications. The high tail in distribution C corresponds to the discriminator firing a second time for larger pulses, on correlated after-pulses about 30 nsec after the initial pulse, an effect largely eliminated in B. As will be seen in Sec. VI. A, the effect is even more apparent when considering the photon-counting statistics. It can be seen, however, that quantum efficiency measurements result in an apparent quantum efficiency of 4.5%, much higher than is the case when proper construction is used.

A list of the ratios of the observed to the expected variances, and the values of b obtained from these re-

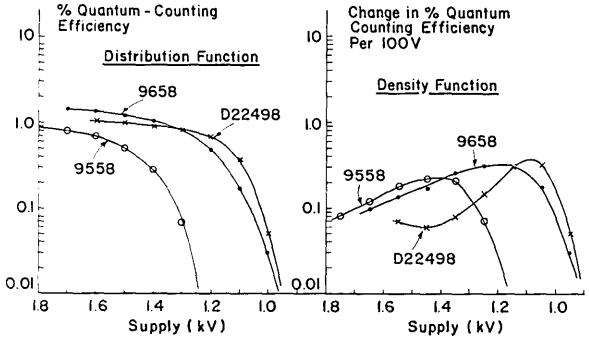

Fig. 4. Distribution and density functions for an EMI 9558B, a 9658A, and a D22498.

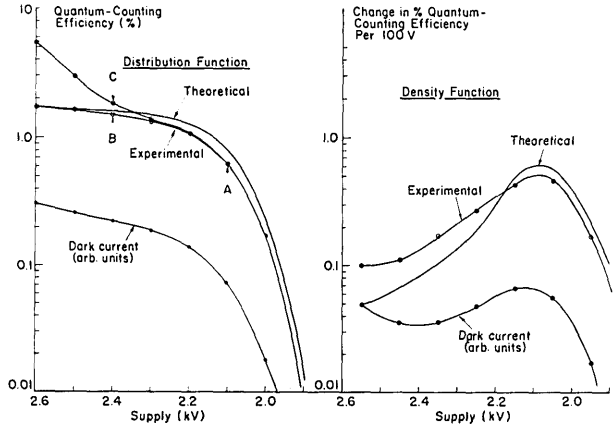

Fig. 5. Distribution and density functions for a Mullard 56 TVP illustrating the effect of the construction of the resistor chain. The theoretical prediction, assuming Poisson multiplication statistics, is also shown. Point A corresponds to good photon-counting statistics, point B corresponds to slight correlations, and point C to marked correlations caused by poor base construction.

Table I. The Effect of the Pulse Height Distribution on the Signal-to-Noise-in-Signal Ratio Attained in Analog Measurements

Photo-multiplier	μ	$\frac{\text{var}(g)_{\text{observed}}}{\text{var}(g)_{\text{Poisson}}}$	b	$\frac{F_{\text{Poisson}}}{F_0}$	$\frac{F_{\text{observed}}}{F_0}$
9558	3.5	2.1	0.3	0.78	0.63
9658	3.2	1.9	0.3	0.76	0.63
D22498	3.3	1.3	0.09	0.77	0.71
56 TVP	5	1.2	0.04	0.83	0.81
FW 130	5	1.0	0	0.83	0.83

sults using Prescott's analysis[15] [see Eq. (11)] is given for various tubes in Table I. In addition, the correction factor,

$$\frac{F}{F_0} = \left[1 + \frac{\text{var}(g)}{\langle g\rangle^2}\right]^{-\frac{1}{2}},$$

is given, both for var(g) calculated assuming Poisson secondary emission characteristics, and for var(g) $\langle g\rangle^2$ having the measured value. It can be seen, from the values of b, that those tubes with focusing properties (e.g., the ITT FW 130 and Mullard 56 TVP) have apparently more uniform secondary emission characteristics than tubes with nonfocusing Venetian-blind structure. The D22498 has a focusing electrode between cathode and first dynode, not present in the 9558 or 9658, in order to adjust the effective cathode area; thereafter it has Venetian-blind structure. This initial focusing may account for the low value of b, indicating that much of the excess variance may arise in the first stages. Comparison of the differential distributions for the different tubes (Figs. 2–5) illustrates the greater width, and hence departure from uniform, Poisson, secondary emission statistics, of the Venetian-blind photomultipliers. The results of Table I can be compared with those obtained by Prescott[15] in his analysis of the data of Bertolaccini and Cova,[1] and Evrard and Gazier,[4] for 56 AVP photomultipliers, and of Delaney and Walton,[2] for an EMI 9514A photomultiplier. For the 56 AVP, which differs from the 56 TVP only in having a different photocathode response, Prescott obtained a value for b of approximately 0.05 over a range of stage gains, in good agreement with this result for the 56 TVP. The comparison is only approximate, since the 56 TVP was not used with uniform gain per stage, though the error involved is only slight. For the EMI 9514, a Venetian-blind photomultiplier, he obtained a value of 0.2 for b. This is consistent with the results obtained here for the 9558 and 9658, each operated with equal gain per stage.

The RCA 7265 gave a much poorer SER, as has also been observed by Pearl.[35] The RCA C70045C, a development tube, showed considerable promise but only functioned for about 50 h, so little real evaluation could be performed.

Generally speaking, it was found that the photomultipliers tested gave rise to pulse height distributions showing a definite peak, and, in many cases, having a shape close to that predicted assuming uniform, Poisson, secondary emission characteristics. In other cases, the excess variance could be attributed to nonuniformity of the dynode surface causing a spread in the mean gain. Another possibility has been demonstrated by Khlebnikov *et al.*[8] who have shown that a nonpeaked, pulse height distribution could be caused by positive ion feedback setting in before the gain of the tube was great enough for all the photoelectrons to be detected. This could be the cause of the poor SER observed for the RCA 7265, since it has been shown[22] that this tube had large positive ion after-pulsing.

V. Measurement of the Quantum Efficiency

A. Cathode Quantum Efficiency

It has been shown above [Eq. (13)] that the over-all quantum efficiency is given by $\alpha = \eta F$. Measurements are made of each of these three quantities independently in the present work.

Measurement of cathode radiant sensitivity, and hence η, is a standard technique using an illumination of $\sim 10^{-2}$ lm from a source at 2870 K color temperature. This is approximately equivalent to 5 μW at 6328 Å. Under normal operative conditions, light fluxes of 10^{-2}–10^{-3} μW (6328 Å) are used to gain a measurable dc output current. Thus, using the standard technique, it is necessary to operate the first one or two stages only as a photocell, electrically connecting the remaining dynodes to act as the anode, otherwise the tube will be damaged by excessive currents. This method has been recommended in the IRE standards[16] and is generally used. The cathode radiant sensitivity is then assumed to be constant over several orders of magnitude and the result is taken to be applicable to normal operating conditions. No measurements of the cathode radiant sensitivity under normal light illumination have been published, probably because of the difficulty of detecting photocurrents of $\sim 10^{-11}$ A in the presence of attendant leakage currents.

In our measurements, normal light fluxes were used and both the cathode and anode radiant sensitivities were measured concurrently, in order to calculate the apparent gain of the tube. An incident light flux of approximately 0.003 μW (6328 Å) gave cathode currents of $\sim 10^{-11}$ A and anode currents of $\sim 10^{-5}$ A. The cathode current was measured using a Millivac picoammeter; the anode current was measured with a model IX Avometer. Conventional measurements of the cathode radiant sensitivity would entail cathode currents of $\sim 10^{-8}$ A. In attempting to measure cathode currents of $\sim 10^{-11}$ A, it was found that only the EMI 9658 and the ITT FW 130 had sufficiently good cathode insulation to give leakage currents of less than 10^{-12} A. In these two cases, for which measurements were possible, the values of cathode radiant sensitivity obtained were in close agreement with the manufacturer's measurements made with photocurrents

Table II. Summary of Photomultiplier Data Relating to Quantum Efficiency

Photomultiplier	Quantum counting efficiency α (%)	Tube[d] voltage (kV)	Cathode radiant sensitivity [mA/W (6328 Å)]	Cathode quantum efficiency (%)	Collection efficiency measurements: $F = \alpha/\eta$	F_0 (Schottky method)	F_0 Corrected for SER variance	Schottky digital method	Current measurement	Anode radiant sensitivity (10^5×A/W)	Tube voltage (kV)	Apparent gain $\langle g \rangle$ (×10^7)	Actual gain (×10^7)
9558	0.8	1.7	15	3.0	0.27	0.5[a]	0.3[a]	0.25	—	2.2[c]	1.4	1.5	5.4
9658	1.45	1.7	32[c]	6.3	0.23	~0.5[a]	0.3	—	0.29	0.27[c]	1.1	0.084	0.37
D22498	1.1	1.6	15	3.0	0.37			—	—	2.4[c]	1.1	1.5	4.1
56 TVP	1.7	2.6	17	3.3	0.51	0.65[b]	0.53	—	—	11.5	2.1	6.7	13
FW 130	0.49	2.25	15[c]	2.9	0.17	—	—	—	0.18	0.49[c]	1.8	0.33	1.9
7265	1.7	2.7	24	4.7	0.36	—	—	—	—	0.22	2.5	0.092	0.25
C70045C	>1.2	5.8	22	4.3	>0.28	—	—	—	—	0.41	5.8	0.19	0.67

[a] Lodge[21] and present work.
[b] Evrard and Gazier.[4]
[c] Manufacturer and present work.
[d] Amplification as in Table V.

of 10^{-8} A. In every case, including those with cathode leakage, the anode radiant sensitivity agreed equally well with the manufacturer's determination. These measurements justified the assumption of linearity made in the stated values of cathode radiant sensitivity. However, since this is usually measured at the peak of the S-20 spectral response, ~4200 Å, this result has to be converted to a value at 6328 Å, introducing an uncertainty of ~20% into the comparison. A summary of the cathode and anode radiant sensitivities, at this wavelength, and the apparent gain g_{app} is given in columns 5, 10, and 12 of Table II.

The interpretation of the cathode quantum efficiency is not completely straightforward, since many of the electrons emitted from the cathode may result from reflection of the incident light off the dynode structure after passing through the photocathode. Thus it is likely that a high percentage of the photoelectrons will not originate on the axis on the multiplier and so will not be collected by the first dynode. If this were the case, one would expect that the collection efficiency for small aperture systems would be lower than that for large aperture systems, in both cases the cathode quantum efficiency is the result both of initial photoemission and also of photoemission on reflection; for small aperture systems, the latter photoelectrons would not be multiplied.

B. Collection Efficiency

The collection efficiency can be calculated from measurement of the signal-to-noise-in-signal ratio using a spectrum analyzer as was shown in Sec. II. The ratio was shown to be [Eq. (21)]:

$$\frac{V_S}{V_N} = \left[\frac{m\eta F}{2\Delta f}\right]^{\frac{1}{2}} \left[1 + \frac{\mathrm{var}(g)}{\langle g \rangle^2}\right]^{-\frac{1}{2}}.$$

If we assume, while making a measurement, that the effect of the shape of the gain distributions is only minor [i.e., assume $\mathrm{var}(g) \simeq 0$], then the value of the ratio obtained, and hence the calculated collection efficiency, will be too high by a factor $[1 + \mathrm{var}(g)/\langle g \rangle^2]^{\frac{1}{2}}$. It has been pointed out elsewhere[36,37] that, if one assumes that the pulse height distribution is that obtained for Poisson secondary emission characteristics, then this correction factor becomes approximately

$$(1 + 1/\mu)^{-\frac{1}{2}} \sim 0.9 \qquad (27)$$

for typical values of the gain per stage. However, in Table I it has already been shown that the correction factor can be considerably greater than this. Therefore, measurements made using the general assumptions of either uniform pulse heights or Poisson secondary emission characteristics will give misleading results for the collection efficiency. The IRE standards,[16] assuming that the gain distribution could be ignored, gave a formula for determining the collection efficiency as follows:

$$\log_{10} F = \tfrac{1}{10}[S/\mathrm{var}(S)]_{db} - \log_{10}(S_k W), \qquad (28)$$

where S is the signal, W is the input light power, and S_k is the cathode radiant sensitivity. Any measure-

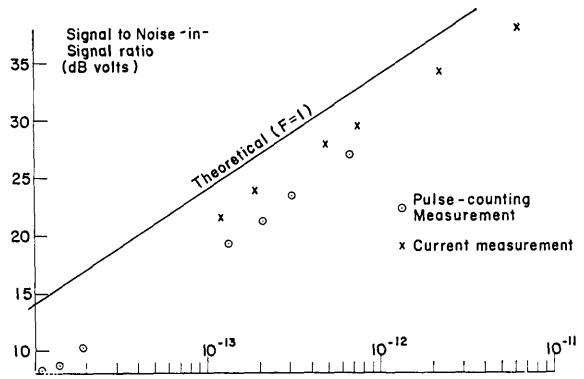

Fig. 6. A comparison of the conventional measurement of collection efficiency, using the signal-to-variance-in-signal ratio of the multiplier output, with that obtained using a standardized multiplier output. The results are compared with the ideal ($F = 1$) ratio.

ments made using this relation are in error by factors that depend on the pulse height distribution but could be at least 2. Table I shows the actual correction factors involved for a selection of the tubes under consideration. Two examples of the importance of this correction factor are shown in columns 7 and 8 of Table II. Measurement of the uncorrected collection efficiency F_0 for various EMI 9558's[21] commonly leads to values of 0.5. When corrected by the relevant factor given in Table I this gives a corrected collection efficiency F of 0.3, which is in good agreement with the value calculated from α and η. Similarly, measurements of F_0 for the 56 AVP[4] gave results of approximately 0.65 for a series of tubes. When corrected F becomes 0.53, in close agreement with the value of 0.51 calculated for a 56 TVP from α and η.

A comparison of measurements in which the effect of the gain distribution is illustrated is shown in Fig. 6. The output of a 9558B photomultiplier is fed into a spectrum analyzer,* first directly through an amplifier, and second after standardization in a discriminator set to accept most of the SER. As can be seen, for a given signal (cathode photocurrent), the effect of ignoring the gain distribution of the nonstandardized pulses was to give a signal to noise-in-signal ratio apparently twice as large as that observed with digital signals. The signal was calculated from measurement of the light input power and knowledge of the cathode quantum efficiency. The result could also be confirmed by measuring the output count rate ($F\eta m$). From these measurements, the uncorrected collection efficiency F_0 is 0.5, in agreement with the result of Lodge.[21] The correct value of F is 0.25, which may be compared with the value of 0.3 calculated from the shape of the gain distribution and from F_0 for this tube. This illustrates the advisability of using digital signals when seeking to measure F. If, on the other hand, it is desired to obtain a good signal to noise-in-signal ratio for a given F, then the use of digital signals gives an improvement in the ratio equal to the reciprocal of the correction factor F/F_0 listed in Table I.

As a final measurement of the collection efficiency, the currents flowing in the cathode, D1 and D2 leads were measured, simultaneously with the anode current, under operating conditions. Obviously, measurements of these currents with the rest of the dynode chain at D2 potential would not give a meaningful value of collection efficiency; one would expect 100%. These measurements were made for the two tubes having no appreciable cathode leakage, the 9658 and the FW 130. The results are compared with the values expected from measurements of the over-all gain per stage in Table III, showing that collection efficiencies for the two tubes are 0.29 for the 9658 and 0.18 for the FW 130, in close agreement with the other available data. Although an appreciable proportion of electrons could well be lost between all the successive dynodes, the probability of the pulse disappearing after the second dynode would be negligible. The effect would be to reduce the apparent gain per stage thereafter.

From Tables II and III, it can be seen that the collection efficiency for the FW 130 is lower than for the other tubes, a fact which is probably related to photoelectrons arising from parts of the photocathode other than a small region round the axis not being multiplied.

Table III. Calculation of the Collection Efficiency by Measurement of the Currents Flowing in the Dynode Leads Under Normal Illumination

Photomultiplier	Gain/stage μ	Current flowing in lead to: Cathode	D_1 Measured	D_1 Calculated	D_2 Measured	D_2 Calculated	Anode	Collection efficiency F
9658	3.5	59	55	147	150	516	60	0.29
FW130	5 (1st) 4 (2nd)	12	18	48	32	180	17	0.18
		pA	pA	pA	pA	pA	μA	

* The correction for measurement of mean square voltage described in Sec. II.B was applied.

Table IV. Normalized Factorial Moments for Coherent Illumination of a 56 TVP Photomultiplier

Normalized factorial moment	10^7 Samples			
	Theory	Exp. *A*	Exp. *B*	Exp. *C*
$n^{(1)}$	1.0000	1.000	1.000	1.000
$n^{(2)}$	1.000 ± 0.001	0.999	1.023	1.063
$n^{(3)}$	1.000 ± 0.002	0.997	1.074	1.321
$n^{(4)}$	1.000 ± 0.003	0.995	1.162	2.365
$n^{(5)}$	1.000 ± 0.012	0.990	1.305	7.205
$n^{(6)}$	1.000 ± 0.036	0.970	1.527	32.52

C. The Over-all Quantum-Counting Efficiency

The over-all quantum-counting efficiency can be measured directly by measurements of the incident light flux and the output count rate. Then α is given by

$$\alpha = \frac{\text{Count rate} \times \text{photon energy}}{\text{incident power}} \times 100\%. \qquad (29)$$

If known neutral density filters and measured light flux* from the laser are used, then the count rates measured in the determination of the pulse height distribution can be calibrated in terms of detector quantum efficiency. This measurement of quantum efficiency is completely independent of knowing the gain. It is only necessary that the gain should be sufficiently large. The correct over-all quantum efficiency is obtained, provided that care has been taken that the discriminator is not firing more than once per pulse, or that the tube itself is not producing too many correlated after-pulses. Both these effects would yield an incorrectly high value of quantum efficiency, as can be seen for case *C* for the 56 TVP photomultiplier (Fig. 5). The ordinates on the pulse height distributions (Figs. 2–5) are accordingly calibrated in terms of the quantum efficiency. Typical values of the maximum quantum efficiency obtained (~1%) were a factor of ~4 lower than the cathode quantum efficiency calculated from the cathode radiant sensitivity. This would correspond to a collection efficiency of only 25%, not 50–70% as has been indicated by other measurements using the method based on the Schottky effect.[4,21]

D. Summary

A summary of all the data obtained relating to quantum efficiency and collection efficiency is given in Table II. The good agreement between the different methods of measurement should be noted. From consideration of the best way to measure the over-all quantum-counting efficiency, or the collection efficiency, it can be seen that current measurement is obviously ineffective since only a few tubes can be assessed this way. The conventional signal to noise-in-signal method gives the incorrect answer and, although it can be corrected from measurements of the SER, it is an involved method using an unnecessary amount of equipment. The good agreement between the corrected value of the collection efficiency and that obtained more directly is probably useful as an indication of the inherent accuracy of the distribution measurements. Both this technique and the use of standardized pulses for the same measurements, based on the Schottky effect, basically consist of measuring $(F\eta m)^{\frac{1}{2}}$ in order to calculate $F\eta m$, a more ponderous, and less accurate, approach than the direct measurement of $F\eta m$. Thus, although the digital technique using a spectrum analyzer leads to the correct result, it involves the use of the spectrum analyzer instead of a scaler, as is used in the direct measurement of $F\eta m$. From a comparison of the methods of measurement, therefore, there seems to be no justification for the use of any method except the direct measurement of photons in and pulses out as a determination of the over-all quantum-counting efficiency. This method has the advantages of using simpler equipment and giving the correct result without any further interpretation.

Measurements have shown, therefore, that, in all the S-20 photomultipliers considered, between 50% and 80% of the photoelectrons leaving the cathode never give rise to pulses at the anode. Thus, any calculations that have been made assuming 100% collection effi-

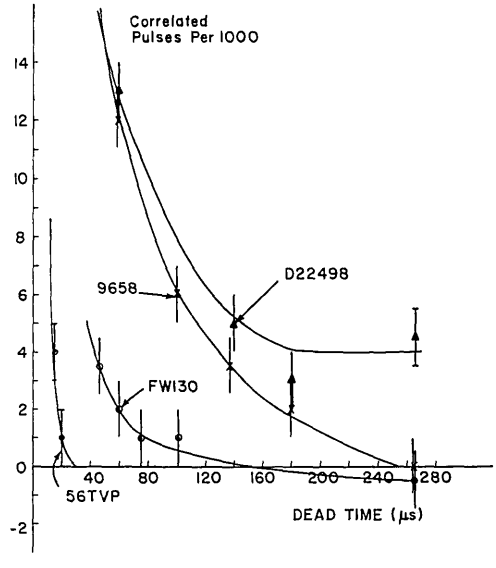

Fig. 7. Variation of the photon-counting correlations with discriminator dead time for the EMI 9658A and D22498, the ITT FW 130, and the Mullard 56 TVP.

* The absolute calibration of laser power meters which are used as secondary standards is a question of some difficulty. We have made independent checks using an Infra-Red Industries standard blackbody source and have no reason to suppose that any large error is being introduced in this way. Many of our conclusions, moreover, are independent of an absolute knowledge of light flux.

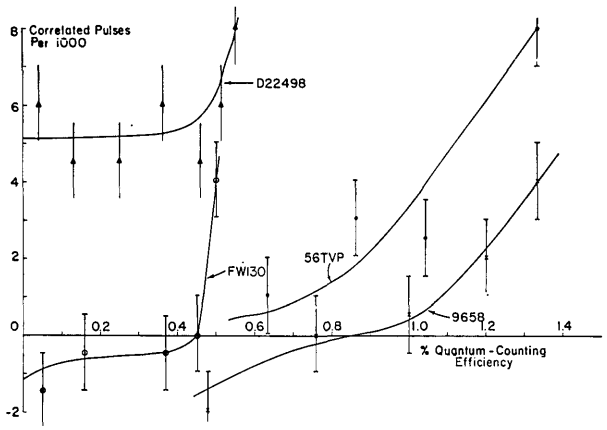

Fig. 8. Variation of the photon-counting correlations with quantum-counting efficiency, obtained by varying the tube voltage, for the EMI 9658A and D22498, the ITT FW 130, and the Mullard 56 TVP.

ciency will be in error. However, calculations based on the measurement of the dc component of anode current will still be correct, though ones based on the variance of this current will not.

VI. Measurement of Time-Dependent Statistical Properties

A. Correlation as a Function of Circuitry

The upper frequency limit on the time-dependent effects that can be observed with a single photomultiplier is determined by the photomultiplier pulse shape. An ideal photomultiplier would have a pulse shape tending to a delta function. Real multipliers, on the other hand, give pulses of finite width, with back edges having overshoots and other undesirable effects that will cause the subsequent discriminator to fire more than once, thus giving correlations. Suitable selection of dead time can be made such that these correlations become negligible; this dead time then determines the maximum countrate the multiplier will handle. Photon-counting measurements have shown that while it is possible to correct for the system dead time[38,39] correlations make the interpretation of results virtually impossible.[22] Such measurements can be used to investigate any effect causing correlations in the times of arrival of the output pulses. The investigation of photon-counting statistics is the most sensitive method of detecting such correlations.

In Table IV, the normalized factorial moments of the photon-counting distributions, measured under three different situations A, B, C (see Fig. 5), are given. It has already been shown that poor base construction (C) results in a distorted pulse height distribution. From Table IV, it can be seen how marked are the effects on the statistics. Experiment B, with the modified capacitor arrangement, gives near Poisson statistics, while at A, the statistics are Poisson within the experimental uncertainties, calculated from the theory of Jakeman and Pike.[40] Another source of correlations is pulse pile-up giving an increased probability of detecting a signal sitting on the tail of the previous one. There are also possible sources of correlated after-pulsing in the tubes themselves involving times of several microseconds. In addition, external amplification always has a deleterious effect on both the SER and the photon-counting statistics; the latter being much more sensitive. Thus, the photon-counting equipment can be used for finding the optimum values of external amplification, tube gain, and system dead time for which the quantum efficiency is a maximum and the observed correlations a minimum.

B. Correlation as a Function of Dead Time

The variation of photon-counting correlations with dead time, for coherent illumination from a Spectra-Physics 119 He–Ne laser, is shown for the EMI 9658 and D22498, the ITT FW 130, and the Mullard 56 TVP in Fig. 7. These measurements show that the 56 TVP can be used for photon counting with a dead time of 20 nsec; the FW 130 requires 75 nsec, the 9658 200 nsec, and the D22498 tends to an asymptotic limit of 4–5 correlated pulses per 1000 at dead times greater than 200 nsec. Thus, the D22498 is unsuitable for photon-counting statistical work. It seems likely that these correlated pulses, which occur more than 0.3 μsec after the initial pulse, which has a full width at half-maximum of about 30 nsec, could be caused by positive ion after-pulsing of a few per 10^5. Since the highest repetition rate, and hence the shortest correlation time, that can be measured depends on the minimum usable dead time, Fig. 7 shows that the 56 TVP was the best photomultiplier to use for high repetition rates. The RCA C70045C (not shown here), however, gave good photon-counting performance with a dead time of only 10 nsec. The RCA 7265 reached an asymptotic limit of about 2 correlated pulses per 100 at a dead time of 16 nsec, probably due to 1 per 1000 positive ion after-pulses.[22] Thus, this tube also is of little value for photon-counting statistical work. The EMI 9558 was similar to the 9658 giving satisfactory photon-counting with a dead time of 200 nsec.

C. Correlation as a Function of the Supply Voltage

The variation of correlations with tube voltage, and hence quantum efficiency, of the multipliers is shown in Fig. 8. As the tube voltage was increased, correlations began to appear due to the inevitable after-pulses becoming sufficiently large to fire the discriminator. A summary of the photon-counting properties of these tubes is given in Table V columns 1–6. Figure 9 illustrates anticorrelations that appeared as a function of the count rate. There was a reduced probability of detecting a pulse immediately following another due to a decrease in the gain per stage. This drop could have been caused by effects such as the drop in the voltage across the later dynodes when large pulses left them

Table V. Summary of Photomultiplier Photon Counting and Dark Count Properties

Photomultiplier	External amplification	Tube voltage (kV)	Dead time (ns)	Quantum-counting efficiency α (%)	Correlated pulses per 10^3	Dark count rate at 0°C (counts per 30 sec)	Dark count (0°C) per 1% quantum efficiency	Cathode area (cm^2)	Dark count rate (0°C) per unit Q.E. per unit area	Lowest dark count rate/1% Q.E. (counts/sec)
9558	×100	1.525	200	0.55	<1	1999	3636	13.5	269	45[a]
9658	×100	1.4	200	1.1	<1	3623	3294	13.5	244	—
D22498	×100	1.13	>200	0.50	5	86	96	0.29	331	—
56 TVP	×10	2.1	20	0.63	<1	1785	2833	13.5	210	71
FW 130[b]	×100	2.15	75	0.46	<1	6	13	0.05	260	1.1
RCA7265	×10	3.0	>16	1.6	25	—	—	—	—	—
C70045C	×8	6.0	10	1.2	<1	—	—	—	—	—

[a] Rodman and Smith.[33]

[b] This tube may be purchased with cathode areas down to 10^{-5} cm^2 with consequently lower dark count rates (~1/sec at room temperature).

taking a certain length of time to recover. As would be expected if this were the cause, the effect could be reduced by using lower count rates or by increasing the tube voltage, provided that the latter did not introduce correlations. Thus, for any tube operating in its optimum photon-counting setting, there is a maximum count rate, lower than that expected from pulse-width considerations, beyond which the statistical distribution is distorted. This limit can be increased by providing constant voltage supplies, such as cathode followers, to the later dynodes instead of the usual resistor chain, to maintain the voltage and hence the gain per stage. It was always found advisable to operate with large currents in the resistor chain, particularly for high gain tubes when high count rates were being detected, and, because of the power dissipated, we often house the resistor chain in a separate box from the multiplier connected by decoupled coaxial cables.

VII. Measurement of the Dark Current Properties

A. The Temperature Dependence

In the previous section, factors providing the upper limit to the count rate were considered. The lower limit is provided by the dark count rate and its variance, observed when the photomultiplier is not illuminated. The dependence of the dark count rate, or dark current, on temperature has been investigated by many authors[5,6,11,13,33,36,37]; the count rate asymptotically approaches a minimum at about −30°C. A typical cooling curve, for a 56 TVP is shown in Fig. 10, where $\log (n/T^2)$ is plotted against $1/T$; n is the number of counts in a fixed time interval, T is the absolute temperature. The higher temperature region from room temperature to 0°C, in which the dependence is linear, shows that the dark count rate obeys Richardson's law, and, therefore, that the dark current is thermionic in origin. The gradient of the linear portion should be the work function of the photocathode, but, as has often been observed[6,11] the value for the work function derived in this way is lower than that calculated from the cutoff of the spectral response of the photocathode. At temperatures below −30°C the count rate appears to become independent of temperature, a result explicable by several mechanisms including importantly a residual, nonthermal dark count rate due to radioactivity in the photocathode or envelope material.

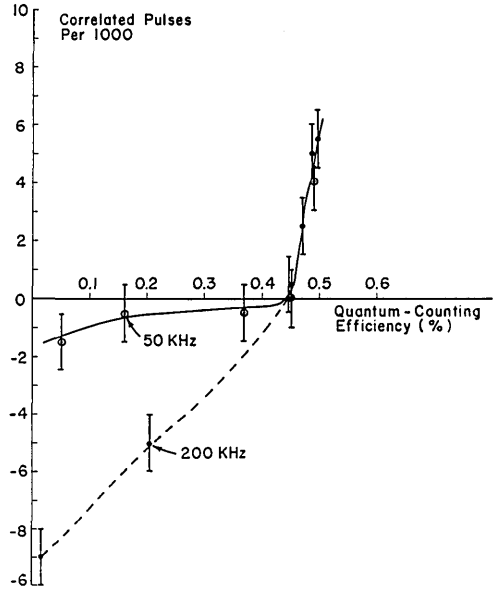

Fig. 9. Anticorrelations in the photon-counting statistics as a function of count rate and quantum efficiency (tube voltage).

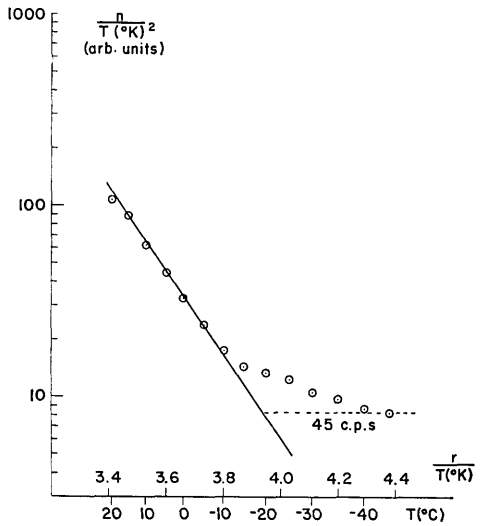

Fig. 10. Cooling curve for the 56 TVP to illustrate the initial cooling following Richardson's law tending to an asymptotic lower limit.

The pulse height distributions and time-dependent statistics of both the room temperature and cooled dark current need to be investigated in order to assess the performance of each tube. The dependence of dark count rate on temperature is shown in Table V, columns 7–11.

B. The Dark Count Pulse Height Distribution

The pulse height distribution of the dark counts of an FW 130 photomultiplier as a function of temperature have been investigated by Oliver and Pike.[6] The SER's for the cooled, and room temperature, dark counts for this FW 130 (No. 116611) were found to be essentially the same as for the light count rates (Fig. 2), demonstrating that in both cases electrons were being produced at the cathode. However, comparison with the SER's of another FW 130 (No. 126620) shows that this is not always the case (Fig. 3). The increasing value of the dark count density function at room temperature for tube 126620 toward higher supply voltages, and hence lower pulse heights, is consistent with electrons being emitted from the first dynode. The cathode was accordingly biased positive with respect to the first dynode, so that electrons leaving the cathode were not multiplied. The dark count rate was then approximately 25% of that measured when contributions from both cathode and D1 were included. Cooling the photomultiplier showed that the dark count rate from D1 was essentially thermal, very few counts being observed when cool. When cooled the pulse height distribution of the residual dark counts of the tube was also the same as the light counts distribution indicating that essentially all the residual counts originated at the cathode. The difference between the two tubes was probably due to the deposition of cathode material on D1 or, more probably, the aperture electrode, during the manufacture of 126620. A third FW 130 (No. 036701) gave a very low dark count rate from D1 at room temperature, indicating very slight contamination with photocathode material. The dark count rate SER for the 56 TVP (Fig. 5) showed a rise toward higher tube voltages probably due to the same effect. Thus, although ideally one would expect similar pulse height distributions for light and dark count,[5,6,8] the process of manufacture can result in their being different.[1] Where the distributions differ, the use of upper and lower level discrimination would improve the signal-to-dark count ratio.[41,42]

C. The Dark Count Time Dependent Statistical Properties

In order to measure signals with rates comparable with the dark count rate, it is necessary to know the variance of this dark count rate. Oliver and Pike[6] have shown that the dark counts of an FW 130, both cooled and at room temperature, had Poisson photon-counting statistics, i.e., the output pulses were randomly distributed in time. Other authors investigating different photomultipliers[13,33] found some evidence of departure from Poisson statistics for the cooled dark counts, but not for those at room temperature. The dark count statistics of the 56 TVP showed that both when the tube was cooled and at room temperature there was an appreciable departure from Poisson statistics. Table VI is a comparison of the normalized, factorial moments of the dark counts for an FW 130 (Ref. 6) and for a 56 TVP. For Poisson statistics, these moments should all be unity. The errors quoted are the theoretical uncertainties due to the finite number of samples.[40] The FW 130 lies within these errors, whereas the 56 TVP is about two standard deviations from the correct value at room temperature, and shows

Table VI. Photon-Counting Statistics of the Dark Current for a 56 TVP and an FW 130 Compared with Poisson Statistics

Normalized factorial moment	Room temperature 10^5 samples			Cooled 10^3 samples		Cooled 10^4 samples	
	FW130	56TVP	Theory	FW130	Theory	56TVP	Theory
$n^{(1)}$	1.000	1.000	1.000	1.00	1.00	1.00	1.00
$n^{(2)}$	1.000	1.009	1.000 ± 0.009	1.01	1.00 ± 0.09	1.73	1.00 ± 0.03
$n^{(3)}$	0.999	1.034	1.000 ± 0.017	1.02	1.00 ± 0.17	6.85	1.00 ± 0.05
$n^{(4)}$	0.991	1.088	1.000 ± 0.030	0.97	1.00 ± 0.30	9.94	1.0 ± 0.1
$n^{(5)}$	0.97	1.205	1.00 ± 0.12	—	—	—	—

major correlations when the tube is cooled. For the FW 130, Oliver and Pike[6] suggested that the residual dark count rate could have been accounted for by the radioactive decay of the 40 K in the glass envelope. For the small effective cathode (0.05 cm^2) of the FW 130, this could well give rise in the main to single photoelectrons only from the bursts of Cerenkov radiation in the glass. The 56 TVP had a cathode nearly 300 times larger, giving an appreciable probability of two or more simultaneous photoelectrons being emitted, with a consequently much larger output pulse and hence an increased probability of observing the correlated after-pulses always present.

D. Measurement of Low Light Flux

In order to choose a photomultiplier for the detection of low signal levels, one requires a low dark count rate for a fixed detection efficiency and also well-defined dark count photon counting statistics, preferably Poisson. If these statistics are not known, it is necessary to have a large signal-to-background ratio so that the correction becomes unimportant. In this respect, the FW 130 is more suitable than the 56 TVP. The dark count properties of the EMI 9558B, 9658A, and D22498, the Mullard 56 TVP, and the ITT FW 130 are summarized in columns 7–11 of Table V. From a comparison of the dark count rate per unit quantum efficiency (column 8), it can be seen that the FW 130 was significantly better than the D22498, which in turn was much better than the other tubes for the detection of low light flux. On normalizing to the cathode area, it can be seen (column 10) that all the tubes had similar thermal dark count properties, as would be expected since all had S–20 cathodes. In order to estimate the lowest detectable light flux, a comparison of the absolute dark count rate per unit quantum efficiency is necessary (column 11). The 9658A would be expected to be similar to the 9558B, the D22498 would have approximately 0.025 of the 9558B dark count rate. Thus the D22498 would be a suitable alternative to the FW 130 for the detection of low light levels in conventional spectroscopy in which the dc output is measured and correlations are unimportant.

VIII. Conclusions

Certain photomultiplier properties have been shown to be desirable for photon counting. Other applications make similar, though less stringent, demands. A summary of these important properties and of the performance of the tubes under consideration is given below. (a) There must be few correlations in the output when the cathode is illuminated with coherent light. This requirement was satisfied by the EMI 9558 and 9658, the Mullard 56 TVP, the ITT FW 130, and the RCA C70045C, but not by the EMI D22498 or the RCA 7265. (b) The anode pulses must be as narrow as possible for the tube to be suitable for high pulse counting rates. The most suitable tubes, in order of merit, were C70045C, 7265,* 56 TVP, FW 130, 9558, 9658, and D22498.* (c) For low light level detection, the dark count rate per unit quantum efficiency must be as low as possible. The order of merit was FW 130, D22498,* and 56 TVP, 9658, and 9558. This quantity was not measured for the two RCA tubes but would be similar to the other 5-cm diam tubes. The thermal dark current was shown to be proportional to the effective photocathode area; thus a small cathode is preferable. Such a cathode also produces a smaller residual dark count rate. (d) For the detection of low light levels, and, in particular, for photon counting with weak signals, it is important that the cooled dark count statistics should be Poisson. Only the FW 130 satisfied this condition. (e) Subject to (c) the cathode quantum efficiency should be as high as possible. The tube with the highest value of α at 6328 Å was the 9658 followed, in order, by the 7265,* C70045C, 56 TVP, and D22498,* 9558, and FW 130. (f) Subject to (c) the collection efficiency should be as high as possible. The order of merit was 56 TVP, D22498,* 7265,* C70045C, 9558, 9658, FW 130. (g) If a nonstandardized output from the multiplier is to be used, var(g) should be a minimum, i.e., the pulse height distribution should be close to that predicted by Poisson secondary emission statistics. Tubes with focusing structure had SER's closer to the theoretical predictions than the nonfocusing type.

For photon counting applications, the ideal photomultiplier would have a small cathode when possible since this gives a low dark count rate. In optical spectroscopy using lasers, it is usually unnecessary to have large illuminated areas on the cathode. It is also a major disadvantage to be receiving dark counts from a large cathode area. Indeed, coherence area limitations often involve the use of apertures of less than 0.05 cm so that cathodes larger than the 0.25-cm diam of the standard FW 130 are a great drawback. The manufacturer will supply FW 130 tubes with magnetic focusing giving an effective cathode diameter of 50 μ with room temperature dark count rates of the order of 1 count/sec.

A narrow output pulse is an advantage provided that the rise time remains greater than that of the discriminator. Less gain, with associated amplifier distortion, is necessary with tubes giving a sharp pulse. Pulse width is related to the focusing properties of the dynode structure which determine the transit time spread. Tubes with Venetain-blind structure are at a disadvantage in this respect. Furthermore, it is preferable to use a high gain tube than a low gain tube with external amplification, since the photomultiplier dynode structure makes a better fast amplifier.

The overriding consideration for statistical experiments is that there should be no correlations either of the dark counts or when the cathode is illuminated. This property does not appear to be related to any particular dynode structure; tubes with simple dynode structures (e.g., 9558, 9658) and tubes with focusing structure (e.g., 56 TVP, FW 130) are both free from

* Not suitable for statistical photon counting work.

correlations in the light count rate, whereas other tubes of the same general type are not. If the correlations are, in fact, due to positive ion after-pulsing this is a function of the hardness of the tube vacuum, which could be related to the presence of gas trapped in the dynode structure during manufacture. In some cases, correlations caused by a ringing pulse shape could be improved by changes in the photomultiplier voltage distribution; other internal feedback effects would need changes in the dynode structure itself. Tubes with coaxial-line anode outputs such as the Philips XP1020 give improved performance at high speeds.

References

1. M. Bertolaccini and S. Cova, Energ. Nucl. **10,** 259 (1963).
2. C. G. F. Delaney and P. W. Walton, Nucl. Instrum. Meth. **25,** 353 (1964).
3. E. H. Eberhardt, IEEE Trans. Nucl. Sci. **NS-11,** 48 (1964).
4. R. Evrard and C. Gazier, J. Phys. Appl. **26,** 37 (1965).
5. G. A. Morton, Appl. Opt. **7,** 1 (1968).
6. C. J. Oliver and E. R. Pike, J. Phys. D. **2,** 1459 (1968).
7. J. A. Baicker, Inst. Radio Eng. Trans. Nucl. Sci. **NS-7,** 74 (1960).
8. N. S. Khlebnikov, A. Ye. Melamid, and T. A. Kovaleva, Radio Eng. Electron. Phys. **7,** 488 (1962).
9. J. R. Prescott, Nucl. Instrum. Meth. **22,** 256 (1963).
10. M. Rome, IEEE Trans. Nucl. Sci. **NS-11,** 93 (1964).
11. J. C. Barton, C. F. Barnaby, and B. M. Jasani, J. Sci. Instrum. **41,** 599 (1964).
12. G. C. Baldwin and S. I. Friedman, Rev. Sci. Instrum. **36,** 16 (1965).
13. M. Gadsden, Appl. Opt. **2,** 1446 (1965).
14. W. H. Wright, J. Appl. Phys. **39,** 3492 (1968).
15. J. R. Prescott, Nucl. Instrum. Meth. **39,** 173 (1966).
16. IEEE Publ. No. 62, Inst. Radio Eng. 7.S1, Inst. Radio Eng. Standards on Electron Tubes, Phototubes, 78 (1962).
17. G. A. Morton, RCA Rev. **10,** 525 (1949).
18. R. W. Engstron, R. G. Stoudenheimer, and A. M. Glover, Nucleonics **10,** 58 (1952).
19. E. H. Eberhardt, IEEE Trans. Nucl. Sci. **NS-14,** 7 (1967).
20. E. H. Eberhardt, Appl. Opt. **6,** 359 (1967).
21. J. A. Lodge, EMI Ltd., private communication.
22. F. A. Johnson, T. P. McLean, and E. R. Pike, in *Proceedings of the International Conference on the Physics of Quantum Electronics, Puerto Rico,* P. L. Kelley, B. Lax, and P. E. Tannenwald, Eds. (McGraw-Hill Book Company, Inc., New York, 1966), p. 706.
23. E. R. Pike, Invited lecture to European Physical Society, Nuovo Cimento, to be published.
24. G. A. Morton and J. A. Mitchell, RCA Rev. **9,** 632 (1948).
25. P. M. Woodward, Proc. Cambr. Phil. Soc. **44,** 404 (1948).
26. L. Janossy, Zh. Eksperim. Teor. Fiz. **28,** 679 (1955) [Sov. Phys.–JETP **1,** 520 (1955)].
27. F. J. Lombard and F. Martin, Rev. Sci. Instrum. **52,** 200 (1961).
28. E. Jakeman, C. J. Oliver, and E. R. Pike, J. Phys. A. **2,** 497 (1968).
29. E. Jakeman and E. R. Pike, J. Phys. A. **2,** 115 (1969).
30. E. Jakeman, C. J. Oliver, and E. R. Pike, J. Phys. A. **2,** 406 (1968).
31. F. T. Arecchi, G. S. Rodari, and A. Sona, Phys. Lett. **25,** 59 (1967).
32. R. F. Chang, V. Korenman, and R. W. Detenbeck, Phys. Lett. **26,** 417 (1968).
33. J. P. Rodman and H. J. Smith, Appl. Opt. **2,** 181 (1963).
34. H. G. Jackson, Nucl. Instrum. Meth. **33,** 161 (1965).
35. P. R. Pearl, J. Sci. Instrum. **44,** 797 (1967).
36. A. Lallemand, in *Astronomical Techniques,* W. Hiltner, Ed. (University of Chicago Press, Chicago, 1962), Vol. II, Chap. 6.
37. J. Sharpe, EMI Rep. R/P021 (1966).
38. F. A. Johnson, R. Jones, T. P. McLean, and E. R. Pike, Phys. Rev. Lett. **16,** 589 (1966).
39. F. A. Johnson, R. Jones, T. P. McLean, and E. R. Pike, Opt. Act. **14,** 35 (1967).
40. E. Jakeman and E. R. Pike, J. Phys. A. **2,** 690 (1968).
41. W. A. Baum, in *Astronomical Techniques,* W. Hiltner, Ed. (University of Chicago Press, Chicago, 1962), Vol. II, Chap. 6.
42. E. H. Eberhardt, ITT Appl. Note **E8** (1965).
43. E. H. Eberhardt, ITT Appl. Note **E5** (1964).